

# Multisensor-based Surface Water Quality Monitoring: A Case Study for the Chalkidiki, Greece

Veronika Kopačková-Strnadová<sup>1</sup>, Martin Kýhos<sup>1,2</sup>, Jan Jelének<sup>1</sup>, Giannis Zabokas<sup>3</sup>, Athina Agali<sup>3</sup>, Kostas Gounaris<sup>3</sup>

<sup>1</sup>Czech Geological Survey, Klárov 131/3, Malá Strana, 118 00 Praha 1, Czech Republic

<sup>2</sup>CZU, Faculty of Environmental Sciences, Kamýcká 129, 165 00 Prague 6, Czech Republic

<sup>3</sup>Hellas Gold, Stratoni, Chalkidiki, 63074, Greece

## Abstract

This study investigates the application of multisource and multiscale Earth Observation (EO) technologies for monitoring water quality in the Kassandra Mining District, Chalkidiki, Greece. We integrate spectral data from various platforms: high-resolution water spectral libraries from an OceanOptics STS-VIS-VIS spectrometer (337–823 nm) on a DJI Phantom 3 UAV, multispectral imagery from a Parrot Sequoia camera (4 bands) on a DJI Phantom 4 Pro UAV, and 8-band multispectral Planet Labs satellite data at 3-meter resolution. These datasets are combined with in situ surface water samples from field campaigns and long-term monitoring by Hellas Gold (HG). Initial results indicate that Total Suspended Solids (TSS), serving as a proxy for estimating arsenic high/medium/low (As) levels, can be predicted at high accuracy using Partial Least Square Regression (PLSR) on the water spectral libraries ( $R^2 = 0.85$ ). Modified spectral indices based on the most important wavelengths identified by PLSR achieved an  $R^2$  of 0.82, while original multispectral indices from PlanetScope imagery yielded an  $R^2$  of 0.78. These findings suggest strong potential for utilizing these data and methods in water quality monitoring at local and regional scales.

**Keywords:** Mine water tracer test, Tyrol/Austria, underground mine, density stratification, lessons learned

## Introduction

Water monitoring is a crucial task for mining companies. Mining operations can affect local water resources, so regular monitoring is vital for ensuring compliance with environmental regulations. Additionally, water quality assessments are essential for pollution prevention, allowing companies to identify contamination from potentially toxic metals or toxic chemicals early on. Immediate corrective actions can then be taken to prevent broader environmental damage affecting ecosystems and public health (Mogimi *et al.* 2024).

Remotesensing techniques offer numerous advantages in water monitoring, including comprehensive coverage, cost efficiency, and real-time monitoring capabilities. Imaging spectroscopy presents an effective alternative to traditional laboratory analyses, enabling

the detection of various environmental parameters, such as total suspended solids (TSS), using spectral sensors (Adjovu *et al.* 2023). Many case studies focused on surface water quality have primarily utilized satellite data (Wirabumi *et al.* 2021). Additionally, the use of UAV-sensed data has rapidly emerged, highlighting its significant potential for the water pollution monitoring (Guimarães *et al.* 2019, Zeng *et al.* 2017).

In this study, we explored the integration of various UAV-based spectral data and developed spectral models suitable for real-time monitoring of surface water quality. We also evaluated the feasibility of up-scaling these spectral models to match the spectral and spatial resolution of high-resolution multispectral satellite data from Planet Labs, thereby facilitating water monitoring over larger areas.

## Test Site

The study was conducted in the Kassandra Mining District on the Chalkidiki Peninsula in northern Greece, known for its rich mineral resources. It hosts one active underground mine, one underground mine in care and maintenance and one open pit / unground mine under construction, all operated by Hellas Gold (HG): Olympias, Stratonis, and Skouries. Olympias primarily extracts gold (Au), lead (Pb), and zinc (Zn), focusing on gold and base metal production. Stratonis specialized in lead (Pb), zinc (Zn), and silver (Ag), establishing itself as a key silver producer; however, it is currently under maintenance. Skouries, which focuses on copper (Cu) and gold (Au), serves as an important source of these minerals but is currently under construction.

## Data

This section outlines the field data acquisition methods, including UAV-based and water sampling, conducted from April 11th to 17th, 2024, in the Kassandra Mining District of Chalkidiki (Fig. 1).

### *UAV-Based Water Spectral Data Acquisition*

The lightweight OceanOptics STS-VIS spectroradiometer (40 mm × 42 mm × 24 mm, 60 g) was mounted on a DJI Phantom 3 UAV to acquire water spectral libraries, capturing data across 1,024 spectral bands

in the 337–823 nm range with an optical resolution of 1.5 nm and a 25° field of view (FOV). Powered by an external battery and operated with a Raspberry Pi 3, it features a Wi-Fi-enabled web interface for ground control. A custom 3D-printed mount was designed for optimal weight distribution and stability. Data were collected at 15 sites (Fig. 1) across three rivers and streams, flying at 3 meters above the water for minimal disturbance and achieving a spatial resolution of 1.2 meters. Data were systematically collected at two-second intervals along three transects: 50 meters upstream, 50 meters downstream, and diagonally across each water body. A customized Python script in Jupyter Notebook processed the radiance data from \*.txt files, calculating final reflectance using input files for dark body, white reference, and sample measurements per the OceanView manual. The Savitzky-Golay filter (SGF) was applied to smooth the collected spectra using the 'scipy.signal.savgol\_filter' function in Python.

Concurrently, multispectral imagery was captured at 13 sites near the mining pits using a lightweight (72 g) Parrot Sequoia camera mounted on a DJI Phantom 3 UAV. This 4-band sensor operates in the Green, Red, Red Edge, and Near-Infrared (NIR) ranges and was paired with a 35-gram sunshine sensor to measure incident solar radiation. Data were collected at 35 meters altitude, with 11-meter line spacing and 2-second

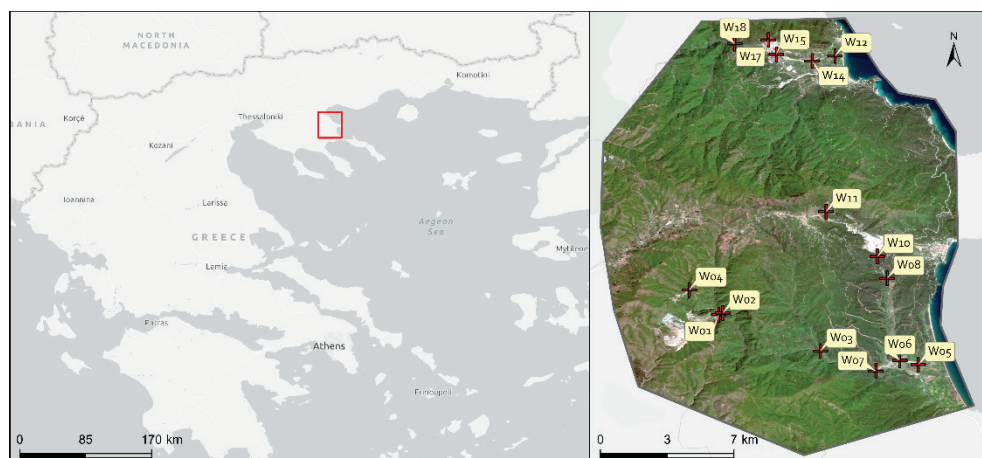


Figure 1 Areas of the interest: Water Quality sampling and UAV data acquisition sites.



capture intervals to ensure adequate overlap. Calibration images were recorded before each flight with an Airnov VIS-NIR greyscale calibration panel. All multispectral data were processed and calibrated using Agisoft Metashape Professional, resulting in high-resolution mosaicked reflectance images (2.5 cm) for detailed spatial insights into the study sites.

### *Satellite Data*

An 8-band multispectral surface reflectance mosaic from PlanetScope, harmonized to the Sentinel-2 sensor, was obtained in GeoTIFF format (Planet Labs PBC, 2024). This mosaic, acquired on April 11th, was specifically chosen to align with the UAV data collection timeframe. The data were accessed through the PlanetScope Explorer platform under a student scientific license.

### *Water in-situ samples*

Water samples were collected during fieldwork from April 11th to 17th, 2024, in conjunction with UAV data acquisition at all 15 locations that matched the UAV sites (Fig. 1), including sections of the Olympias, Stratoni, and Skouries streams in active mining areas. These samples were analyzed at HG laboratories for the same parameters as in long-term monitoring, including potentially toxic metals and Total Suspended Solids (TSS) concentrations. However, organic carbon, another important water quality parameter, was not possible to analyse at HG laboratories. The results were statistically evaluated to identify key relationships relevant to water quality assessment. Additionally, we examined long-term environmental data from the HG monitoring system, covering January 2015 to April 2024, which includes a wide variety of parameters also analyzed in the April 2024 water samples.

## **Methods**

### *Statistical analysis of laboratory water analysis*

A common statistical assessment was applied to the in-situ water sample data, which included correlation analysis, linear regression, and calculation of the coefficient of determination.

### *Partial Least Squares Regression (PLSR)*

To assess the high-spectral resolution data from the OceanOptics STS-VIS (water spectral libraries), Partial Least Squares Regression (PLSR) was employed. PLSR is a quantitative chemometric method designed to analyze data with strong correlations and noise. Its main advantage over other multivariate methods is its ability to manage datasets with more variables than samples, making it ideal for spectroscopic data containing hundreds to thousands of reflectance values. PLSR utilizes two matrices: X (independent variables, such as spectral libraries) and Y (dependent variables, such as chemical laboratory analyses). It applies a technique similar to Principal Component Analysis (PCA) to reduce the dimensionality of the X matrix while maximizing its covariance with Y.

### *Band indices*

PLSR was conducted on the OceanOptics STS-VIS high-spectral resolution data (water spectral libraries) to identify spectral wavelengths most strongly correlated with selected water parameters. The most sensitive wavelengths were then used to modify existing multispectral indices, including the Normalized Difference Vegetation Index (NDVI; Rouse *et al.*, 1973), Normalized Difference Water Index (NDWI; McFeeters, 1996), Normalized Difference Suspended Solids Index (NDSSI; Hossain *et al.*, 2010), and Water Ratio Index/ red-band modification (WRI; Shen and Li, 2010). These indices were applied to imaging data from the multispectral Parrot Sequoia and PlanetScope sensors; however, NDSSI was not calculated for the Parrot Sequoia due to its lower spectral resolution. Finally, water indices from all three datasets were statistically analyzed using linear regression to assess their relationships with the tested water parameters.

## **Results**

### *Selection of the water environmental indicators*

After analyzing laboratory results, TSS was the only optically active constituent (OAC)

that consistently exceeded detection limits across most samples, showing significant variation among sampling sites. A linear regression analysis revealed a correlation between TSS and As values ( $R^2 = 0.33$ ), which improved after excluding samples with low TSS (<5 mg/L) and As (<15  $\mu\text{g/L}$ ) concentrations, leading to high RMSE values. With these thresholds, the correlation strengthened, achieving an  $R^2$  of 0.43 and 0.44 for both water sample analysis and long-term monitoring, respectively (Fig. 2). These findings suggest that TSS can serve as a proxy for estimating arsenic concentrations (Nasrabati *et al.* 2018), enabling predictions of low, medium, and high As levels based on TSS measurements.

### Spectral data analysis

PLSR was applied using high-resolution spectral data from water spectral libraries. In this analysis, reflectance served as the independent variable (X), while TSS and As were the dependent variables (Y). The derived regression coefficients (Fig. 3a-b) indicated that wavelengths from the red to near-infrared regions were the most significant for predicting TSS as well as for As. Consequently, a PLSR model was established for TSS prediction, achieving an  $R^2$  of 0.99 for the training dataset and  $R^2$  of 0.85 for the validation dataset (Fig. 3c) using the Leave-One-Out method (Kopačková-Strnadová *et al.* 2021). In the case of As, we could only

establish a training model, achieving an  $R^2$  of 0.97 (Fig. 3d). Unfortunately, validation was not feasible due to the dataset lacking representative values that fall in the middle range between low and high values.

To assess the estimation of TSS, potentially also As, using spectral indices, four commonly used multispectral indices were adapted to suit the high spectral resolution of the water spectral libraries. Rather than broader spectral regions for the blue, green, red, and near-infrared bands, we used wavelengths most sensitive to TSS, identified by PLSR: 460.5 nm, 530.7 nm, 674.2 nm, and 805.9 nm (Tab. 1). These spectral indices were then also applied to images from the Multispectral Planet using the original spectral bands (Tab. 1). For Parrot Sequoia images, the NDSSI index wasn't used due to the limited number of spectral bands available.

When comparing the regression results between the in-situ data and the analyzed spectral datasets (Tab. 2), the water spectral libraries—characterized by high spectral resolution and high spatial detail—to those obtained from multispectral imaging data, it is evident that models with higher  $R^2$  values were achieved using the water spectral libraries. However, this trend does not hold for the NDSSI index, which seems that may perform better with broader wavelength ranges (e.g., spectral bands) as it was specifically designed for multispectral data. This will be the focus of further analysis. Overall,

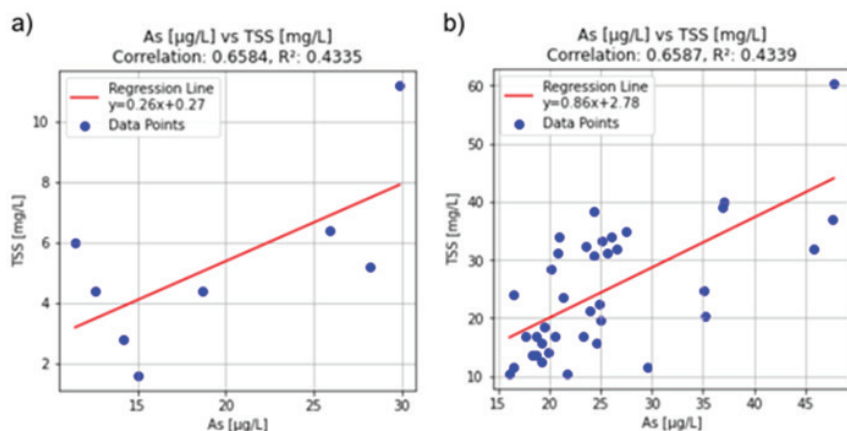


Figure 2 Correlation between TSS and As: 2024 In-situ samples,  $r=0.66$ ,  $R^2=0.43$  (a), Long-term monitoring 2015-2024,  $r=0.66$ ,  $R^2=0.44$  ( $p < 0.001$ ) (b).

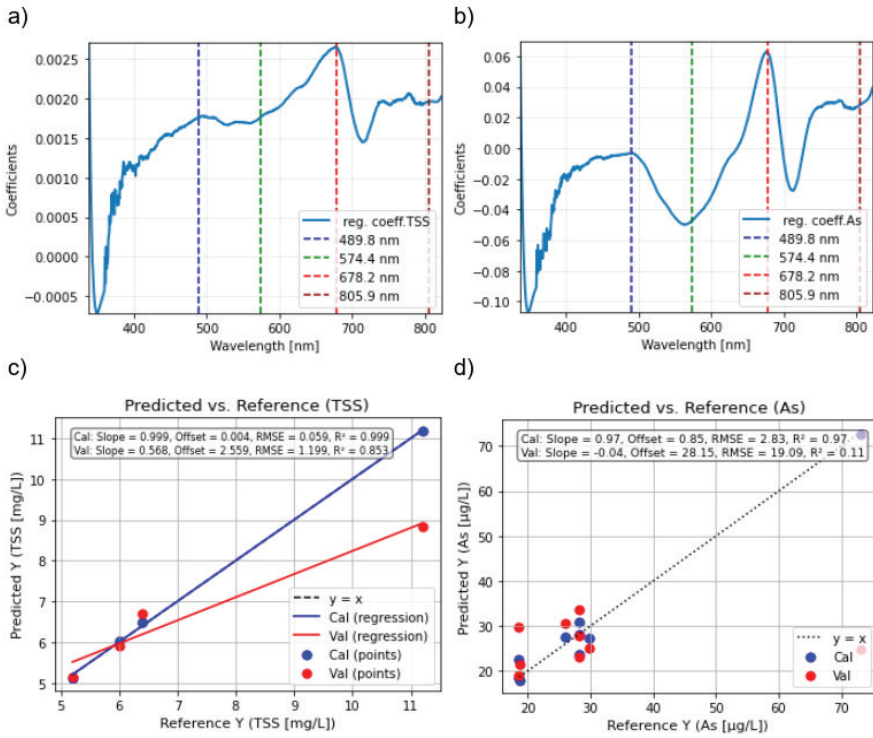


Figure 3 PLSR analysis and predictions applied to high-resolution spectral data - water spectral libraries: (a) Regression coefficients for TSS prediction, (b) Regression coefficients for As prediction, (c) PLSR predictions for TSS (blue – calibration, red – validation), and (d) PLSR predictions for As (blue – calibration, red – validation).

Table 1 Indices definition and adjusted formula used for the water spectral libraries/STS-VIS data.

Indices	Standard formula	Reference	Adjusted formula to STS-VIS data
NDVI	$\frac{\rho_{NIR} - \rho_{RED}}{\rho_{NIR} + \rho_{RED}}$	Rouse <i>et al.</i> , 1973	$\frac{\rho_{805.9} - \rho_{674.2}}{\rho_{805.9} + \rho_{674.2}}$
WRI (Red)	$\frac{\rho_{GREEN} - \rho_{RED}}{\rho_{NIR} + \rho_{RED}}$	Shen and Li, 2010	$\frac{\rho_{530.7} + \rho_{674.2}}{\rho_{805.9} + \rho_{674.2}}$
NDWI	$\frac{\rho_{GREEN} - \rho_{NIR}}{\rho_{GREEN} + \rho_{NIR}}$	McFeeters, 1996	$\frac{\rho_{530.7} - \rho_{805.9}}{\rho_{530.7} + \rho_{805.9}}$
NDSSI	$\frac{\rho_{BLUE} - \rho_{NIR}}{\rho_{BLUE} + \rho_{NIR}}$	Hossain <i>et al.</i> , 2010	$\frac{\rho_{460.5} - \rho_{805.9}}{\rho_{460.5} + \rho_{805.9}}$

Table 2 Statistical evaluation of the linear regressions performed between water in-situ analysis and the spectral indices from the water spectral libraries (STS-VIS), Parrot Sequoia, and Planet Lab data.

Indices	R <sup>2</sup> /Regression		
	STS-VIS data	Parrot Sequoia	Planet Lab data
NDVI	0.815 / y = 0.05x – 0.09	0.721 / y = 0.11x – 0.51	0.493 / y = 6.11x + 1.76
WRI	0.731 / y = -0.02x + 1.02	0.309 / y = -0.08x – 1.76	0.647 / y = -18.49x + 17.60
NDWI	0.781 / y = -0.02x + 0.01	0.623 / y = -0.07x + 0.58	0.775 / y = -23.49x – 2.83
NDSSI	0.288 / y = -0.10x – 0.09	X	0.715 / y = -24.00x – 3.93

reliable TSS predictions were obtained when scaling the tested indices to Planet Lab and Parrot Sequoia data, with the NDWI index achieving the highest  $R^2$  of 0.78 and 0.62 respectively.

## Conclusion

This study examined the feasibility of estimating Total Suspended Solids (TSS) correlated with arsenic (As) using high spectral and spatial resolution data, specifically water spectral libraries (STS-VIS) and multispectral imaging data from PlanetScope. The results confirm the significant potential of these contactless technologies for water quality monitoring, leading to the following conclusions: a) TSS is an important parameter correlating with As ( $r = 0.66$ ,  $R^2 = 0.44$ ,  $p < 0.001$ ), indicating TSS can serve as a proxy for semiquantitative As estimations (high-medium and low values); b) TSS predictions can achieve an  $R^2$  of 0.85 using PLSR on the water spectral libraries; c) Generally good predictions were observed with multispectral indices and PlanetScope data (Fig. 4), with the NDWI yielding the best results ( $R^2 = 0.78$ ).

## Acknowledgment

The presented analysis was conducted under the support of the EC grant MultiMiner. The MultiMiner project is funded by the European Union's Horizon Europe research and innovation actions programme under Grant Agreement No. 10109137474.

## References

- Adjovu, G.E., Stephen, H., James, D., Ahmad, S., 2023. Measurement of Total Dissolved Solids and Total Suspended Solids in Water Systems: A Review of the Issues, Conventional, and Remote Sensing Techniques. *Remote Sensing* 15, 3534.
- Hellas Gold S.A., 2016. Environmental Monitoring Program. Available at: <https://environmental.hellas-gold.com/> [Accessed 20 Jul. 2024].
- Hossain, A. K. M. A., Jia, Y., & Chao, X. (2010, September). Development of remote sensing based index for estimating/mapping suspended sediment concentration in river and lake environments. In *Proceedings of 8th international symposium on ECOHYDRAULICS (ISE 2010)* (Vol. 435, pp. 578-585).
- Jackisch, R., Heincke, B. H., Zimmermann, R., Sørensen, E. V., Pirttijärvi, M., Kirsch, M., ... & Gloaguen, R. (2021). Drone-based magnetic and multispectral surveys to develop a 3D model for mineral exploration at Qullissat, Disko Island, Greenland. *Solid Earth Discussions*, 2021, 1-51.

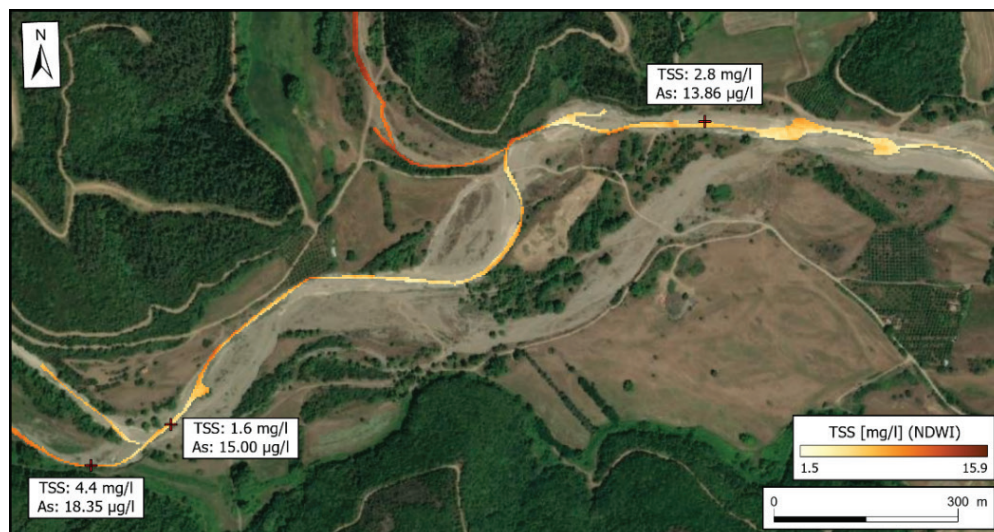


Figure 4 TSS estimated employing NDWI to PlanetScope data (11th of April 2024, Skouries).



- Kopačková-Strnadová, V., Rappich, V., McLemore, V., Pour, O., & Magna, T. (2021). Quantitative estimation of rare earth element abundances in compositionally distinct carbonatites: Implications for proximal remote-sensing prospection of critical elements. *International Journal of Applied Earth Observations and Geoinformation*, 103, 102423
- McFeeters, S. K. (1996). The use of the Normalized Difference Water Index (NDWI) in the delineation of open water features. *International journal of remote sensing*, 17(7), 1425-1432.
- Planet Labs PBC, 2024. Scene Level Normalization and Harmonization of Planet Dove Imagery. Retrieved from [https://assets.planet.com/docs/scene\\_level\\_normalization\\_of\\_planet\\_dove\\_imagery.pdf](https://assets.planet.com/docs/scene_level_normalization_of_planet_dove_imagery.pdf)
- Rouse, J. W., Haas, R. H., Schell, J. A., & Deering, D. W. (1974). Monitoring vegetation systems in the Great Plains with ERTS. *NASA Spec. Publ*, 351(1), 309.
- Shen, L., & Li, C. (2010, June). Water body extraction from Landsat ETM+ imagery using adaboost algorithm. In 2010 18th International Conference on Geoinformatics (pp. 1-4). IEEE.
- Wirabumi, P., Kamal, M., Wicaksono, P., 2021. Determining effective water depth for total suspended solids (TSS) mapping using PlanetScope imagery. *International Journal of Remote Sensing* 42, 5784–5810.
- Zeng, C., Richardson, M., King, D.J., 2017. The impacts of environmental variables on water reflectance measured using a lightweight unmanned aerial vehicle (UAV)-based spectrometer system. *ISPRS Journal of Photogrammetry and Remote Sensing* 130, 217–230.